AGU ADVANCING EARTH AND SPACE SCIENCE

Water Resources Research

TECHNICAL REPORTS: METHODS
10.1029/2019WR026924

Key Points:
- Extreme rainfall does not scale consistently with surface air temperature
- Integrated water vapor is the most stable covariate when correlated to rainfall
- It is suggested integrated water be used as a covariate for rainfall projection

Correspondence to:
A. Sharma,
a.sharma@unsw.edu.au

Citation:
Roderick, T. P., Wasko, C., & Sharma, A. (2020). An improved covariate for projecting future rainfall extremes. *Water Resources Research*, *56*, e2019WR026924. https://doi.org/10.1029/2019WR026924

Received 8 DEC 2019
Accepted 29 JUN 2020
Accepted article online 4 JUL 2020

An Improved Covariate for Projecting Future Rainfall Extremes?

Thomas P. Roderick[1], Conrad Wasko[2], and Ashish Sharma[1]

[1]School of Civil and Environmental Engineering, University of New South Wales, Sydney, Australia, [2]Department of Infrastructure Engineering, University of Melbourne, Melbourne, Australia

Abstract Projection of extreme rainfall under climate change remains an area of considerable uncertainty. In the absence of geographically consistent simulations of extreme rainfall for the future, alternatives relying on physical relationships between a warmer atmosphere and its moisture carrying capacity are projected, scaling with a known atmospheric covariate. The most common atmospheric covariate adopted is surface air temperature, as it exhibits great consistency across climate model simulations into the future and, as per the Clausius-Clapeyron relationship, has a well-established link to atmospheric moisture capacity. However, empirical assessments of this relationship show that it varies with latitude, surface temperature, atmospheric temperature, and other factors, suggesting there may be more stable "global" atmospheric covariates that could be used instead. We argue that a better-suited covariate would be one that captures the relationship between extreme rainfall and temperature but exhibits greater consistency in the relationship across regions as well as climatic zones. Our analysis identifies plausible atmospheric indicators of changes to future extreme rainfall, which now proliferate literature and compare their suitability based on the variability they exhibit across multiple geographical, topographic, and climatic zones within Australia. It is shown that surface air temperature exhibits a regionally inconsistent relationship with extreme rainfall and hence is not suitable for projecting to future conditions. The study identified integrated water vapor and surface dew point temperature as promising alternatives, with the former showing greater consistency in space but at the cost of reduced temporal coverage.

Plain Language Summary Studies of extreme rainfall sensitivity to temperature (termed scaling) improve our understanding of how extreme rainfall can be expected to change under global warming. The widespread and intuitive use of surface air temperature in rainfall scaling studies is likely the result of its observational availability and its apparent physical relationship with extreme rainfall. This study investigates the reliability of surface air temperature, integrated water vapor, surface dew point temperature, and 850 hPa atmospheric temperature as possible covariates for rainfall projection. Consistent with observed increases in extreme rainfall, a covariate that exhibits consistency across varying climatic conditions will result in more robust projections of future extreme rainfall. Here, we investigate the susceptibility of each covariate to varying conditions exhibited by the broad climates found across Australia. Integrated water vapor, retrieved from satellites, is found to be the most suitable scaling covariate for extreme rainfall projection.

1. Introduction

Extreme precipitation presents an enormous risk to infrastructure and human activity. This is compounded by the fact that future extreme rainfall is projected to increase with global warming (e.g., Craig, 2010). Projections are based on the reasoning that as temperature increases, the water holding capacity of the atmosphere increases permitting higher rainfall intensities (e.g., Allen & Ingram, 2002). The Clausius-Clapeyron (C-C) relationship is used to define the maximum water holding capacity of a parcel of air at a given temperature. Previous studies have found that extreme rainfall typically increases at a similar rate to the increase in water holding capacity of the atmosphere (Allen & Ingram, 2002; Roderick et al., 2019; Soden & Held, 2006).

Projecting future rainfall extremes has been attempted by multiple methods, including climate model simulations and using relationships with selected atmospheric indicators of rain. The former, while intuitive, suffers from the known instability that climate models exhibit for future rainfall simulations (Eghdamirad et al.,

2017; Woldemeskel et al., 2015). The latter requires defining a relationship that is motivated through physics and uses atmospheric variables that can be simulated using available climate models. Given the C-C relationship and the relative consistency surface air temperature (SAT) exhibit across climate model simulations of the future (Johnson & Sharma, 2009), many temperature-based projections of extreme rainfall have been attempted (Bürger et al., 2019; Hettiarachchi et al., 2018; Lenderink & Attema, 2015; Manola et al., 2018; Verstraten et al., 2019). These have evolved to alternatives projecting nonstationary intensity-frequency-duration relationships using temperature as a covariate (Agilan & Umamahesh, 2017; Ali & Mishra, 2017; Golroudbary et al., 2019). These approaches, however, have been questioned by many who have pointed to an apparent breakdown in the relationship of temperature and atmospheric moisture holding capacity (from which the extreme rainfall intensity is derived), for low and very high temperatures, most evident in tropical regions (Roderick et al., 2019). Of marked concern is the breakdown in the relationship with high temperatures, as there is a need to project into the future when temperatures will be greater (Chan et al., 2016; Wang et al., 2017). It is important to identify a more suitable atmospheric covariate that is physically defensible, can be obtained using climate model simulations of the future, has reliable observational records, and exhibits a more regionally consistent relationship with extreme rainfall than temperature. This forms the focus of the investigation reported here.

Our study examines what atmospheric covariate should be used to project extreme rainfall into the future. It argues that for any single covariate to be adopted as the basis of projecting extreme rainfall, it must satisfy certain conditions. First, there must exist a physical basis behind choosing the covariate, or an argument that a stable relationship between extreme rainfall and the covariate, even in extrapolation, should exist. Second, one should have reliable projections of the covariate using climate model simulations across the world, ideally without the necessity of downscaling them to finer spatial resolutions. Third, the covariate should have a stable empirical relationship with extreme precipitation, stability defined on the basis of consistency across regions, altitudes, climate types, and analogous factors. Lastly, as the covariate is likely to assume values in the future that it has not been observed in the past, the empirical relationship should also exhibit stability across the tails of the covariate marginal probability distribution where change will occur.

Here we assess alternatives for suitable atmospheric covariates based on the rationale above, and a network of 109 high-quality daily rainfall stations across multiple climatic zones, elevations, latitudes, and longitudes in Australia. The rest of the paper is as follows. We next discuss the considerable literature there exists on the topic of choosing a suitable atmospheric covariate for projecting extreme rainfall, including the findings that have motivated our study. This is followed by a presentation of the methods and the data used in section 3, following which results are presented (section 4). The next section delves into the results from a physical perspective, reasoning what relationship one should expect with each of the alternatives considered in our study. This is followed by the conclusions derived from the paper.

2. Background

Past investigations on the changes in extreme rainfall rely on the C-C "scaling" rationale. This is motivated through the expression for a change in extremes (P) as a function of time (t):

$$\frac{\partial P}{\partial t} = \frac{\partial P}{\partial T} \times \frac{\partial T}{\partial t}. \tag{1}$$

The second term in 1 represents the scaling which is the rate of change of a hydrological extreme with a suitable covariate (in this case temperature T). The rationale here is that the third term in 1 is positive since the start of the previous century and the expectation is that it will remain so, allowing a time trend in the extreme variable of interest to be ascertained.

Assuming extreme rainfall occurs when the atmosphere is approaching its moisture carrying capacity allows one to ascertain its rate of change with temperature (Trenberth, 2011; Trenberth et al., 2003). Empirical estimates, especially for higher percentiles, become possible as temperature presents itself as a nonunique variable (unlike time). Furthermore, using the C-C relationship, one can ascertain theoretical values of this scaling, which has been shown to theoretically range from 6–7%/K for the case of extreme rainfall (Westra et al., 2014).

Using a global daily rain gauge data set, annual maxima were found to have a linear association with global mean temperature of 5.9% to 7.7%/K (Westra, Alexander, et al., 2013), similar to the C-C relationship, matching climate model projections for extreme rainfall (Zwiers et al., 2013). Similar associations between temperature and the historical rate of increase in extreme rainfall have been found in a continental study of the United States (Barbero et al., 2017) and a more localized study in Japan (Fujibe, 2013). These associations have generally been formulated using average global (or continental) temperatures (Lenderink & Attema, 2015). When local temperatures are used, this association diminishes, suggesting local temperatures do not reflect the overall moisture budget responsible for extreme precipitation (Barbero et al., 2017; Wasko & Nathan, 2019). Hence, the theorized C-C relationship frequently does not match empirically calculated extreme rainfall-surface temperature scaling.

Global studies have repeatedly also found negative scaling in the low-latitude locations (Utsumi et al., 2011; Wasko et al., 2016). Lenderink and van Meijgaard (2008) concluded that the C-C relationship holds below 8–10°C, and a higher than C-C rate is found for warmer temperatures. A shift toward convective storms has been proposed to explain the varying scaling results (Haerter & Berg, 2009). Trenberth et al. (2003) proposed above C-C or "super" C-C scaling rates as physically plausible due to the release of latent heat, allowing the storm to expand its area from which it sources moisture (Lenderink et al., 2017; Lochbihler & Lenderink, 2017; Peleg et al., 2018; Trenberth et al., 2003).

Wang et al. (2017) found a "peak" temperature, beyond which scaling rates switch to negative. This is consistent with Hardwick Jones et al. (2010), who found extreme precipitation intensity to scale with temperature above the C-C relationship only up to 20–26°C, with a negative scaling observed above this. Drobinski et al. (2016) have found that multiple climate and geographical factors can result in the scaling rate differing from the expected C-C relationship. These include time and spatial averaging, precipitation efficiency, and most importantly land surface profile. Others have attributed the negative scaling in dry regions to the increased sunlight received on low rainfall days, thus drying the upper soil moisture and resulting in a higher SAT (Trenberth & Shea, 2005).

Ali and Mishra (2017) have proposed that the negative scaling results are due to a "cooling" effect of rainfall, resulting in a reduced local air temperature on the day of rainfall. A larger precipitation event is reasoned to produce a stronger cooling effect on the local air temperature, thus resulting in the apparent negative scaling. Bao et al. (2017) takes credence away from the cooling theory as it was shown that taking the SAT, preceding the rainfall event had little influence on the scaling rate. Fujita and Sato (2017) have explained the apparent difficulties of scaling rainfall with SAT by examining the relationship between tropospheric water vapor content and SAT. Precipitable water vapor is found to scale variably with SAT, depending primarily on the temperature itself (Fujita & Sato, 2017). Finally, the negative scaling rate obtained in the tropics has been attributed to the limitation of temperature due to evaporation; this conclusion being based on an assessment of satellite measures atmospheric moisture data over the locations studied (Roderick et al., 2019).

Previous research has consistently used SAT as the covariate to scale extreme rainfall intensity (Agilan & Umamahesh, 2017). This includes the use of SAT as a covariate for nonstationary rainfall intensity-frequency-duration curves (Agilan & Umamahesh, 2017; Ali & Mishra, 2017) and the use of SAT indirectly as a covariate in continuous rainfall simulation (Wasko & Sharma, 2017a) and rainfall disaggregation (Bürger et al., 2019; Westra, Evans, et al., 2013). Engineering design guidelines in Australia (Bates et al., 2019) recommend the long-term consideration of scaling with SAT in the prediction of future rainfall intensity-frequency-distribution (IFD) where risks are nonnegligible.

The variance and irregularity of SAT scaling bring into question the use of SAT as a global scaling covariate for modeling future extreme rainfall, as extremes appear to be increasing uniformly across world (Westra, Evans, et al., 2013; Zhang et al., 2019). This widespread use of SAT is likely due to the substantial quantity of observational records available for analysis. SAT however is unlikely to be a suitable covariate to scale rainfall intensity due to the consistently "sub" and "super" C-C scaling rates found and it not being a direct measure of atmospheric moisture.

To overcome the limitations of using SAT for scaling calculations, Ali and Mishra (2017) proposed scaling extreme rainfall intensities with 850 hPa tropospheric air temperature (T850) from reanalysis products and observations of dew point temperature (DPT). Both tropospheric air temperature and DPT were

found to scale positively and closer to the C-C rate than scaling with SAT (Ali & Mishra, 2017). Atmospheric air temperature and DPT were suggested as suitable nonstationary covariates for the scaling of extreme rainfall (Golroudbary et al., 2019) with DPT performing better than atmospheric air temperature (Bui et al., 2019). Surface DPT measurements taken prior to rainfall events have been used as a scaling covariate to find a 14% per degree dependency, approximately twice that of the C-C relation (Lenderink et al., 2011), and in general are found to be more likely to result in positive scaling when compared to the use of SAT (Ali et al., 2018; Lenderink & van Meijgaard, 2010; Panthou et al., 2014; Park & Min, 2017; Wasko et al., 2018). Since DPT is a measure of the absolute humidity of the atmosphere, it has been championed as possible covariate for projecting precipitation extremes. DPT measurements from both observation data and climate models have been used successfully to project increasing local precipitation extremes (Lenderink & Attema, 2015; Manola et al., 2018). Additionally, probable maximum precipitation estimates have been made taking advantage of surface DPT (Hansen et al., 1988).

In this paper we investigate the suitability of four different covariates for the projection of extreme rainfall in future conditions. SAT is compared to (surface) DPT, integrated water vapor (IWV), and T850. IWV has been proposed as a covariate from its relative accuracy in global climate models (GCMs) (Shi et al., 2014). Previous studies have relied heavily on climate models to retrieve atmospheric variables due to the difficulty in obtaining atmospheric observations. This study has retrieved the Atmospheric Infrared Sounder (AIRS) satellite data for observational estimates of IWV and T850 (Aumann et al., 2003; Tobin et al., 2006). The AIRS satellite data provide the opportunity to calculate extreme rainfall scaling with atmospheric moisture content. It is expected that an ideal covariate will be informative of future expected extreme rainfall and be independent of varying geographical factors and climate.

3. Data and Methods

We use daily surface rainfall, daily SAT, and daily DPT data from the Australian Bureau of Meteorology weather station data set. A total of 109 weather stations were identified to provide a reasonable spatial coverage across a broad range of climates with complete data records from 2002 to 2015 (to match the satellite observations). Rainfall observations are taken at 9:00 am daily and include the precipitation for the 24-hr period preceding the measurement. The daily SAT is calculated by averaging the minimum and maximum temperature in the 24 hr preceding the 9:00 am measurement. Station data were included if over 97% of records are flagged for acceptable record quality.

The AIRS satellite data (Version 6) give a global gridded data set from 2002 to current day providing twice daily measurements of temperature and moisture. AIRS data are publicly available for academic research at National Aeronautics and Space Administration (NASA; http://acdisc.gsfc.nasa.gov/opendap/Aqua_AIRS_Level3/). It measures moisture and air temperature remotely, providing data for 100 atmospheric pressure levels on a 1° by 1° grid. This covers the entire globe with a 12-hr pole-to-pole orbit that takes two daily measurements at 01:30 and 13:30 hr. IWV and T850 observations are retrieved for each day. IWV is in degrees kg m^{-2} and T850 is in degrees K. The two daily measurements have been averaged to provide an indicative average daily value. The AIRS data achieve 1 K root mean squared errors in 1 km layers below 100 hPa for temperature and 10 K root mean squared errors for moisture concentration when compared to alternate satellite data sources (Divakarla et al., 2006). The AIRS temperature and moisture observations are generally in agreement with radiosondes measurements (Divakarla et al., 2006).

The AIRS data have been paired to the surface observations of daily rainfall, SAT and DPT. This has been performed by identifying the 1° by 1° AIRS grid cell in which the weather station resides. The resulting database contains 109 stations with daily rainfall, daily average SAT, daily IWV, daily average DPT, and daily average T850.

Quantile regression is used to assess the scaling rate of rainfall intensity with each covariate. Quantile regression provides a statistical tool to calculate the scaling rate that is unbiased of bin size (Wasko & Sharma, 2014). With each weather station's daily data, we can directly calculate the scaling rate using quantile regression (Koenker & Bassett, 1978). The following description of quantile regression follows from Hao and Naiman (2007).

Consider a set of data pairs (x_i, y_i) for $i = 1,\ldots,n$. The quantile regression can be expressed as

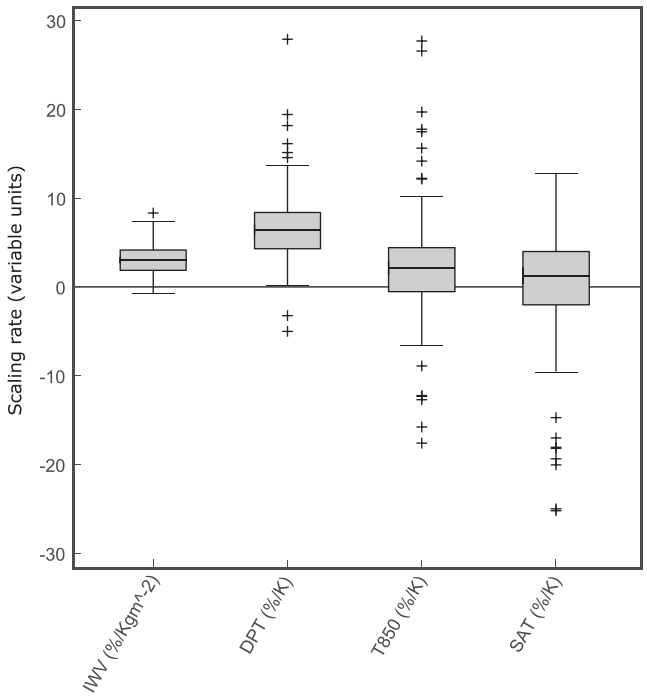

Figure 1. Boxplots representing the probability distribution of derived scaling rates across all study locations using the 90th percentile of rainfall in quantile regression.

$$y_i = \beta_0^{(p)} + \beta_1^{(p)} x_i + \epsilon_i^{(p)}, \tag{2}$$

where $0 < p < 1$ is the quantile and ϵ_i is an error term with zero expectation. The parameters $\beta_0^{(p)}$ and $\beta_1^{(p)}$ are chosen to minimize the residual error measure D:

$$D\left(\beta_0^{(p)}, \beta_1^{(p)}\right) = p \sum_{y_i \geq \beta_0^{(p)} + \beta_1^{(p)} x_i} |y_i - \beta_0^{(p)} - \beta_1^{(p)} x_i| + (1-p) \sum_{y_i < \beta_0^{(p)} + \beta_1^{(p)} x_i} |y_i - \beta_0^{(p)} - \beta_1^{(p)} x_i|. \tag{3}$$

Quantile regression differs from linear regression, as it minimizes the absolute deviation of the errors with a weighting of p for under prediction and $(1 - p)$ for over prediction.

For this study the slope of the relationship is given by $\beta_1^{(p)}$ for the (90th percentile) scaling rate of all daily rainfall values above 1 mm. For rainfall, we have taken the log of the daily measurements in mm as proposed by Lenderink and van Meijgaard (2008). The slope $\beta_1^{(p)}$ is transformed $100 \times (e^{\beta_1^{(p)}} - 1)$, resulting in a scaling rate with units % increase/decrease per Kelvin when scaling rainfall against temperature. This is alike for DPT and T850, as they share common units. For scaling rainfall intensity against IWV, the units are % increase/decrease in rainfall per unit increase in IWV (kg m^{-2}). Equivalently, the percentage increase for a ΔT Kelvin increase in temperature is given by $100 \times \left[\left(1 + \beta_1^{(p)}\right)^{\Delta T} - 1\right]$.

To assess stability in the sample scaling coefficient estimates, the following procedure is used. First, a set of regional markers is defined for each location, which are latitude, longitude, elevation, mean temperature (for all temperature measures considered), mean rainfall, and the mean square error of the quantile regression estimate of the scaling coefficient. As the desired outcome here is the lack of a systematic regional pattern in the scaling coefficient, the probability of a casual dependence with each regional marker is then ascertained. This is accomplished by estimating a nonparametric information theoretic measure of dependence, the partial information correlation (PIC), which equates to the absolute value of the partial correlation in the case of Gaussian random variables. The PIC is derived from the partial mutual information (PMI) between the scaling estimates with respective regional markers. The rationale behind the PMI is a measure of dependence captured by the ratio of the joint and the product of marginal probabilities for the variables whose dependence is being ascertained, the two equaling each other (and canceling out in the ratio) if the variables are independent. Readers are referred to relevant publications (Sharma & Mehrotra, 2014; Sharma et al., 2016) for additional details and to the user manual for the NPRED software (Sharma et al., 2016) that was used to ascertain the significance level (p value) of the estimated PIC. For a scaling covariate to be adopted there must exist a high probability of independence with any of the site-specific factor considered (Barbero et al., 2018).

4. Results

4.1. Geographic and Climatic Variability of Covariates

A box plot of extreme rainfall scaling values for all the weather stations studied with each respective covariate is given in Figure 1. A median of 1.3%/K is obtained for scaling rainfall against SAT, 3.1% kg^{-1} m^2 for IWV, 7.2%/K for DPT, and 2.1%/K for scaling rainfall against T850. The calculated scaling rates show a relatively large spread for SAT and T850 across Australia with a considerable number of outliers. More consistent results are found for the extreme scaling rainfall with IWV and DPT.

The negative values for the lower SAT scaling rates are largely a result of the tropical stations in Australia's north, biasing the overall result negatively (Roderick et al., 2019). This negative scaling is also evident for T850 with the 25th quantile of scaling rates being −0.5%/K. IWV and DPT have substantially less variability in their calculated scaling rates across the varying climates of Australia, supporting the suitability of IWV and DPT as covariates for the prediction of extreme rainfall.

Table 1
PIC Estimates for Scaling Coefficients and Plausible Indicators of Systematic Variability

	SAT	IWV	DPT	T850
Latitude	0.75	0.00	0.00	0.59
Longitude	0.52	0.00	0.22	0.40
MSE	0.68	0.00	0.25	0.47
Mean (IWV)	0.71	0.01	0.00	0.57
Mean (SAT)	0.70	0.00	0.35	0.54
Mean (DPT)	0.47	0.24	0.24	0.47
Mean (T850)	0.72	0.00	0.23	0.56
Elevation	0.00	0.00	0.00	0.27
Mean (P)	0.31	0.00	0.55	0.36

Note. "P" here denotes annual precipitation, while "MSE" denotes the mean squares error from the quantile regression estimate of the scaling coefficient, other terms being as defined elsewhere. A partial information correlation (PIC) of 1 indicates dependence between the scaling estimate and associated indicator. The 5% one-sided significant PIC indicative of a nonzero estimate is 0.19.

To identify the regional effect on the calculated scaling rate of extreme rainfall, the PIC (Sharma & Mehrotra, 2014; Sharma et al., 2016) was estimated for a range of plausible covariates. The PIC here represents a measure of nonlinear dependence between the scaling coefficient and an indicator, a value of zero reflecting no dependence while a value of 1 reflecting perfect dependence. As can be ascertained from the results in Table 1, little dependence is exhibited by both IWV and DPT with the indicators considered. In contrast, SAT has significant dependence with each of the indicators, implying it systematically varies across the locations used. This systematic variation makes it an unsuitable indicator to compare across locations, while the two low PIC coefficients exhibit markedly greater suitability. While there is uncertainty in the results as these are based on 109 locations alone, the suitability of IWV and, to a reduced extent, of DPT, over the other scaling coefficients is clear.

4.2. The Relative Sensitivity of Estimated Scaling Coefficients to Extreme Precipitation Values

The use of the scaling coefficient in assessing change in extreme rainfall for future warmer climates assumes that the scaling coefficient in itself is invariant with the range of the covariate (temperature or otherwise) used. With a reduced sample size, we would expect higher uncertainty; however, the ideal covariate would exhibit no systematic changes scaling rate to ensure future relevance. To assess this, the following experiment was conducted. The scaling coefficient for each of the cases assessed before was re-estimated progressively increasing the sample size of extreme rainfall observations that were organized with respect to increasing covariate values. To provide some stability in the estimates, the sample sizes were increased from 50% to 100%, and results averaged over all study locations. The outcomes of this analysis are presented in Table 2. As can be seen, the scaling coefficient gradually decreases with temperature-based covariates and exhibits less systematic change with IWV. This outcome can be interpreted to convey that the current sample scaling coefficient estimates may be representative of the relationship between extreme rainfall and the covariate to a better extent into the future with IWV than would be the case with the other covariates considered.

A lower range of calculated scaling rates with varying portions of the covariate rainfall data pairs suggests consistency independent of the magnitude of the scaling value (Table 2). This would allow accurate prediction of rainfall intensity into the future, where an overall increase is expected for all covariates studied. DPT and IWV, proportionally, have the least variation, followed by T850 then SAT.

4.3. Projected Changes in Extreme Precipitation

Given the relative confidence with which each of the considered covariates can be projected into the future using the current generation of climate models available (Eghdamirad et al., 2017; Woldemeskel et al., 2015), an assessment of the implications of using each of the proposed covariates for projecting extreme rainfall at the 109 daily precipitation Australian locations is undertaken. The projected extreme rainfall using SAT, IWV, DPT, and T850, for the year 2081–2100, is presented in Figure 2. SAT is projected to rise 3.7 K as per the RCP8.5 scenario outlined in the Intergovernmental Panel on Climate Change (Collins et al., 2013). DPT has been shown to increase at approximately the same rate as SAT, and therefore, we have assumed a similar indicative value of 3.7 K increase by 2100 (Lenderink & Attema, 2015). A 3.7 K increase is also used for T850, which has been show to increase at approximately the same rate as SAT (Brocard et al., 2013). IWV has been modeled to increase approximately 20–30% by 2100 from assessing the average of seven GCMs for the RCP8.5 scenario (Kunkel et al., 2013). Using the average daily IWV measured over the 13-year time span for all station studied (20.08 k gm^{-2}), and a mean percentage increase of 25% by 2100, we have assumed an increase of 5.00 k gm^{-2} by 2100 for Australia. This matches the theoretical increase

Table 2
The 90th Percentile Scaling Rate Calculated Utilizing Only the Lower % of Each Covariate Observations Out of the Rainfall/Covariate Pairs

	SAT (%/K)	IWV (%/KGM^{-2})	DPT (%/K)	T850 (%/K)
<50%	3.4	4.1	6.3	4.0
<60%	3.3	4.3	5.7	2.7
<70%	3.2	3.9	6.0	3.5
<80%	2.8	3.8	6.1	3.4
<90%	3.1	3.5	6.6	3.2
100%	1.3	3.1	7.2	2.1
Range	2.1	1.2	1.5	1.9

Note. Range is given for all calculations for comparison.

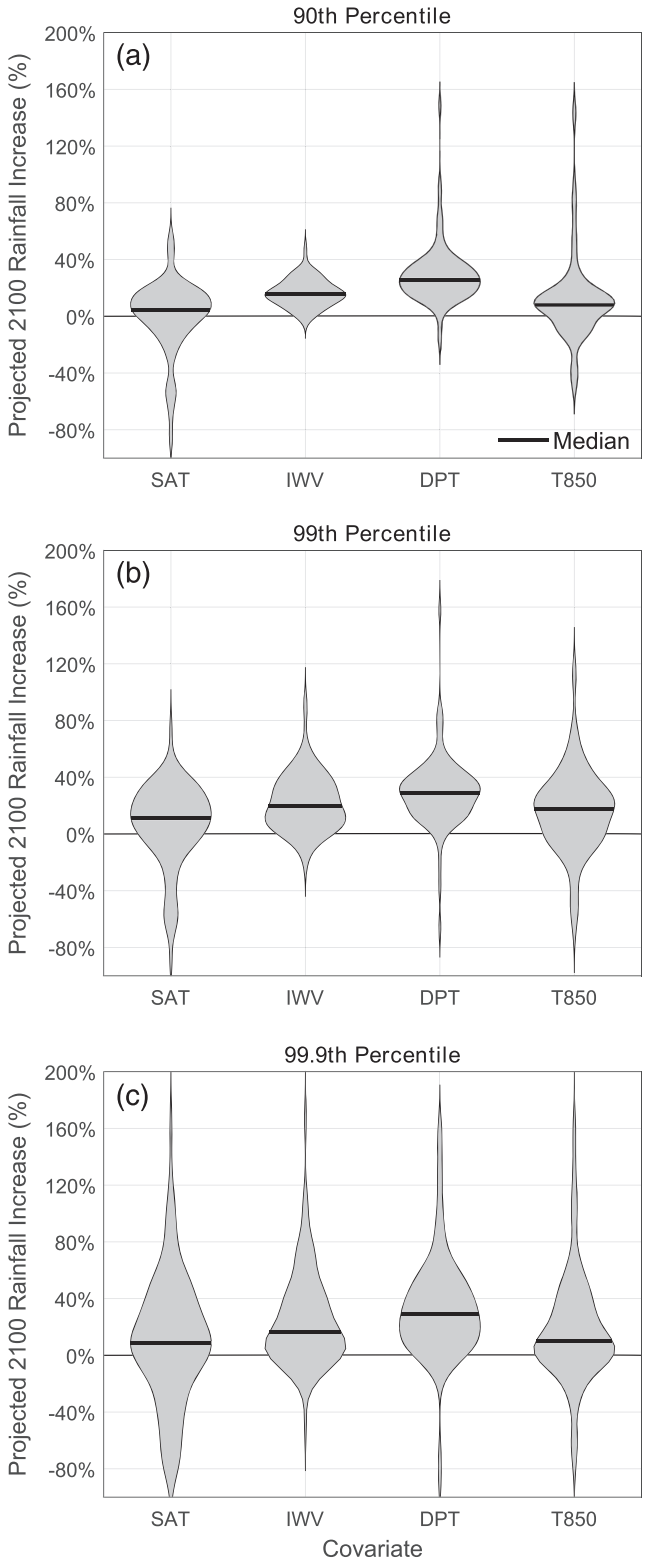

Figure 2. Violin plot of projections of average global extreme precipitation increase for 2081–2100 using different covariates for (a) 90th, (b) 99th, and (c) 99.9th percentiles. Quantile scaling rate estimates are based on the 109 daily weather stations whose data were used in the analysis; 3.7 K increase in SAT, DPT, and T80 assumed by 2081–2100 and 5.00 kg/m^2 assumed for IWV.

in saturation water vapor due to a 3.7 K increase at a background temperature of approximately 298 K.

As a baseline, for the most extreme rainfall, regional climate models (RCMs) project an expected extreme rainfall increase of 7%/K under varying temperature conditions (Ban et al., 2015; Bao et al., 2017; Kendon et al., 2014) for the same study region. However, the increase in precipitation is proportional to how extreme the event is (Pendergrass, 2018; Wasko & Sharma, 2017b). For the events considered here, the 90th percentile of rain days is approximately equivalent to the 99th percentile across all days. The GCM average precipitation increase for the 99th percentile is 4.2%/K with bottom quartile 3.0%/K and top quartile 5.6%/K (Pendergrass, 2018; Pendergrass & Hartman, 2014). This yields an expected increase of 16.4% by 2081–2100 with a 3.7 K increase in temperature under the RCP8.5 scenario (Collins et al., 2013) with 11.6% and 22.3% increases for the bottom and top quartile, respectively.

Our scaling analysis of SAT has found a median value of 4.8% increase in extreme rainfall by 2081–2100 (Figure 2a). This simple comparison with GCM's expected increases highlights the possible inaccuracy of using SAT as a scaling covariate. The SAT scaling values substantially underestimate the GCM expectation of increase in extreme rainfall by 2081–2100 for the majority of the stations studied. T850 performs similarly, with substantial underprediction. IWV scaling across the stations gives a median 16.7% increase in expected future extreme rainfall by 2081–2100, and DPT gives median 29.3% increase (Figure 2a). Using IWV and DPT as covariates for rainfall projection gives systematic increases in the extreme rainfall consistent with expectation and GCM projections. However, when GCM projections are used as a reference, it appears that DPT may overestimate future daily extreme rainfall increases. As rainfall extremes are expected to increase more for more extreme percentiles (Pendergrass, 2018), the results are repeated for the 99th (Figure 2b) and 99.9th percentile (Figure 2c). The results are consistent with the above discussion with greater increases projected for each covariate, albeit with greater uncertainty due to the relatively short data lengths used. IWV scaling appears to show the least spread around the median value showing consistency across the 109 weather stations studied (Figure 2).

5. Discussion

5.1. Theoretical Limitations

The results presented earlier articulate the use of a unified covariate for expressing CC scaling in future studies. The results suggest that the use of temperature may be misleading in establishing a scaling rate and using it to project extreme rainfall into the future and also suggest that dew DPT or the IWV may be better covariates to adopt. This section attempts to reconcile the empirical results presented earlier with our theoretical knowledge of atmospheric moisture holding capacity.

Teten's equation (Monteith & Unsworth, 2008) for saturation vapor pressure (e_s in kPa) is commonly used in hydrometeorological studies to ascertain evaporation and cloud formation. This equation is an empirical approximation of the Clausius Clapeyron relationship, well approximated for temperature (in degrees Centigrade) ranging from 0–50°C, and can be written as

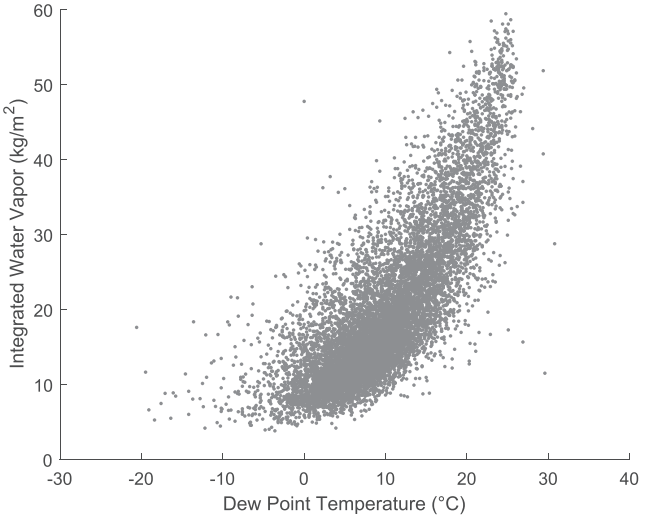

Figure 3. Scatter plot of IWV (kg/m^2) against DPT (°C) for all 109 weather stations from 2002 to 2015.

$$e_s = 0.6108\ exp\left(\frac{17.27 \times T}{(237.3 + T)}\right). \tag{4}$$

Assuming a constant relative humidity leads to its derivative equaling:

$$\frac{1}{e_s}\frac{\partial e_s}{\partial T} = \frac{17.27 \times 237.3}{(237.3 + T)^2}, \tag{5}$$

which takes on values of 7.3%/°C at T = 0°C to 5.3%/°C at 40°C, this term being commonly approximated to 7%/°C and referred to as the C-C scaling rate.

The assumption of a constant relative humidity in the above scaling estimate has motivated the need for using the DPT instead. Note that if an air parcel is at a temperature and vapor pressure of (T, e), it equivalently also exists at (T_d, e_s), where T_d represents the DPT. Hence, use of T_d in 5 results in an actual vapor pressure e, which can be argued to correspond to the actual amount of water present in the air column.

However, both T and T_d represent surface temperature attributes, while the extreme rainfall that is the variable of interest depends largely on the precipitable water within the air column. It is well known that both relative humidity and temperature change significantly with height (Boos, 2012). It has been shown using climate models that the scaling for precipitable water with temperature is theoretically lower (about 5%/°C) than that for extreme precipitation (Boos, 2012).

The question must be asked whether one needs to use surface temperature or DPT to approximate precipitable water if direct measurements of the same can be used instead. While DPT is a better alternative than temperature alone, the fact remains that it represents surface conditions and can thus only offer an approximation to the moisture an atmospheric column contains.

5.2. Limitations of Extrapolatability

The asymptotic relationship observed by DPT observations in relation to IWV is highlighted in Figure 3. DPT appears to approach a limit in magnitude, whereas IWV appears to increase more consistently at higher values. The estimation of future rainfall extremes requires a scaling covariate with a reliable, steady relationship that can be predicted into the future. DPT (similar to T850 and SAT) presents difficulties as it is shown to exhibit some limitation in its relationship, complicating its utilization as a scaling covariate. IWV does not appear to exhibit a limiting relationship with DPT.

6. Conclusions

In this study we have considered SAT, IWV, DPT, and T850 as covariates for projecting future extreme rainfall intensity. SAT has been the primary scaling covariate utilized in previous research to predict extreme precipitation. Consistent with physical reasoning and published literature, both surface and atmospheric variables have been considered. IWV was found to be the least susceptible covariate to influence from the geographical and climate factors examined. Scaling extreme rainfall with daily mean SAT and T850 produced large variability and was highly susceptible to influence from station specific parameters.

The median 90th percentile IWV scaling rate with rainfall intensity is 3.1% kg^{-1} m^2. This rate is reasonably consistent spatially around Australia with varying latitude, longitude, and elevation, as well as the average SAT. Scaling rainfall against DPT also showed low variance though it still exhibits some correlation with latitude and average SAT. DPT is a measure of the atmospheric moisture at surface level, which does not consider the total moisture in the entire vertical air column. This may be the reason IWV showed less influence with latitude and average SAT. Although DPT scaling was found to align with RCM prediction for the most extreme rainfall, its susceptibility to latitude and average SAT may limit its practicality as a global scaling covariate. SAT and T850 did not produce an expectation of global rainfall increase in the vicinity of the climate model projections. This, combined with their susceptibility to background factors and large variability,

limits their usefulness as a scaling value for the prediction of extreme rainfall. Our analysis is based on the simple relationship between atmospheric moisture and rainfall, which likely does not capture the changed storm dynamics due to climate change (Trenberth, 1999) and how they might affect rainfall (Zhang et al., 2017). As SAT has also been used to project subdaily rainfall (Agilan & Umamahesh, 2017), future research is recommended at a subdaily time scale to confirm the stability of scaling rainfall against IWV and examine consistency with observed trends (Zhang et al., 2019).

Our analysis of IWV confirms it as the most stable variable for scaling future extreme rainfall at the daily time scale. Scaling with DPT is a significant improvement on SAT; however, it maintains more influence from climatic factors then IWV. We have found a preference for IWV as a scaling covariate as it gives a consistent regional scaling relationship and is equally informative of the extreme rainfall intensity we can expect in the future. New methods for estimating future rainfall intensities that use IWV instead of SAT or time as covariates (Agilan & Umamahesh, 2016, 2017; Ali & Mishra, 2017; Cheng & Aghakouchak, 2014) should be investigated.

Data Availability Statement

Surface rainfall and temperature data can be obtained from the Australian Bureau of Meteorology and can be found online (at www.bom.gov.au/climate/data/stations/). The AIRS data can be obtained from the NASA Goddard Earth Sciences Data Information and Services Centre (GESDISC) and can be found online (at https://airs.jpl.nasa.gov/data/get_data).

Acknowledgments

Conrad Wasko acknowledges funding from the University of Melbourne McKenzie Fellowship scheme. This research was partially supported by the Australian Research Council. The authors thank Ditiro Moalafhi for assistance with AIRS data.

References

Agilan, V., & Umamahesh, N. V. (2016). Modelling nonlinear trend for developing non-stationary rainfall intensity-duration-frequency curve. *International Journal of Climatology*, *37*(3), 1265–1281. https://doi.org/10.1002/joc.4774

Agilan, V., & Umamahesh, N. V. (2017). What are the best covariates for developing non-stationary rainfall intensity-duration-frequency relationship? *Advances in Water Resources*, *101*, 11–22. https://doi.org/10.1016/j.advwatres.2016.12.016

Ali, H., Fowler, H. J., & Mishra, V. (2018). Global observational evidence of strong linkage between dew point temperature and precipitation extremes. *Geophysical Research Letters*, *45*, 12,320–12,330. https://doi.org/10.1029/2018GL080557

Ali, H., & Mishra, V. (2017). Contrasting response of rainfall extremes to increase in surface air and dewpoint temperatures at urban locations in India. *Scientific Reports*, *7*(1), 1–15. https://doi.org/10.1038/s41598-017-01306-1

Allen, M. R., & Ingram, W. J. (2002). Constraints on future changes in climate and the hydrologic cycle. *Nature*, *419*(6903), 228–232. https://doi.org/10.1038/nature01092

Aumann, H. H., Chahine, M. T., Gautier, C., Goldberg, M. D., Kalnay, E., Mcmillin, L. M., et al. (2003). AIRS/AMSU/HSB on the Aqua Mission: Design, science objectives, data products, and processing systems. *Processing*, *41*(2), 253–264.

Ban, N., Schmidli, J., & Schär, C. (2015). Heavy precipitation in a changing climate: Does short-term summer precipitation increase faster? *Geophysical Research Letters*, *42*, 1165–1172. https://doi.org/10.1002/2014GL062588.Climate

Bao, J., Sherwood, S. C., Alexander, L. V., & Evans, J. P. (2017). Future increases in extreme precipitation exceed observed scaling rates. *Nature Climate Change*, *7*(2), 128–132. https://doi.org/10.1038/nclimate3201

Barbero, R., Fowler, H. J., Lenderink, G., & Blenkinsop, S. (2017). Is the intensification of precipitation extremes with global warming better detected at hourly than daily resolutions? *Geophysical Research Letters*, *44*, 974–983. https://doi.org/10.1002/2016GL071917

Barbero, R., Westra, S., Lenderink, G., & Fowler, H. J. (2018). Temperature-extreme precipitation scaling: A two-way causality? *International Journal of Climatology*, *38*(December 2017), e1274–e1279. https://doi.org/10.1002/joc.5370

Bates, B., McLuckie, D., Westra, S., Johnson, F., Green, J., Mummery, J., & Abbs, D. (2019). Chapter 6. Climate change considerations. Book 1: Scope and philosophy. In J. Ball, M. Babister, R. Nathan, E. Weinmann, M. Retallick, & I. Testoni (Eds.), *Australian rainfall and runoff—A guide to flood estimation*. Commonwealth of Australia.

Boos, W. R. (2012). Thermodynamic scaling of the hydrological cycle of the last glacial maximum. *Journal of Climate*, *25*(3), 992–1006. https://doi.org/10.1175/JCLI-D-11-00010.1

Brocard, E., Jeannet, P., Begert, M., Levrat, G., Philipona, R., Romanens, G., & Scherrer, S. C. (2013). Upper air temperature trends above Switzerland 1959–2011. *Journal of Geophysical Research: Atmospheres*, *118*, 4303–4317. https://doi.org/10.1002/jgrd.50438

Bui, A., Johnson, F., & Wasko, C. (2019). The relationship of atmospheric air temperature and dew point temperature to extreme rainfall. *Environmental Research Letters*, *14*(7), 074025. https://doi.org/10.1088/1748-9326/ab2a26

Bürger, G., Pfister, A., & Bronstert, A. (2019). Temperature-driven rise in extreme sub-hourly rainfall. *Journal of Climate*, *32*(22), 7597–7609. https://doi.org/10.1175/JCLI-D-19-0136.1

Chan, S. C., Kendon, E. J., Roberts, N. M., Fowler, H. J., & Blenkinsop, S. (2016). Downturn in scaling of UK extreme rainfall with temperature for future hottest days. *Nature Geoscience*, *9*(1), 24–28. https://doi.org/10.1038/ngeo2596

Cheng, L., & Aghakouchak, A. (2014). Nonstationary precipitation intensity-duration-frequency curves for infrastructure design in a changing. *Scientific Reports*, *4*(1), 7093. https://doi.org/10.1038/srep07093

Collins, M., Knutti, R., Arblaster, J., Dufresne, J.-L., Fichefet, T., Friedlingstein, P., et al. (2013). Long-term climate change: Projections, commitments and irreversibility. In T. F. Stocker, D. Qin, G.-K. Plattner, M. Tignor, S. K. Allen, J. Boschung, et al. (Eds.), *Climate Change 2013: The Physical Science Basis. Contribution of Working Group I to the Fifth Assessment Report of the Intergovernmental Panel on Climate Change* (pp. 1029–1136). Cambridge, UK and New York, NY, USA: Cambridge University Press.

Craig, R. K. (2010). Stationarity is dead—Long live transformation: Five principles for climate change adaptation law. *Harvard Environmental Law Review*, *34*(1), 9–73.

Divakarla, M. G., Barnet, C. D., Goldberg, M. D., McMillin, L. M., Maddy, E., Wolf, W., et al. (2006). Validation of Atmospheric Infrared Sounder temperature and water vapor retrievals with matched radiosonde measurements and forecasts. *Journal of Geophysical Research*, *111*, D09S15. https://doi.org/10.1029/2005JD006116

Drobinski, P., Alonzo, B., Bastin, S., da Silva, N., & Muller, C. (2016). Scaling of precipitation extremes with temperature in the French Mediterranean region: What explains the hook shape? *Journal of Geophysical Research: Atmospheres*, *121*, 3100–3119. https://doi.org/10.1002/2015JD023497

Eghdamirad, S., Johnson, F., & Sharma, A. (2017). How reliable are GCM simulations for different atmospheric variables? *Climate Change*, *145*(1-2), 237–248. https://doi.org/10.1007/s10584-017-2086-x

Fujibe, F. (2013). Clausius-Clapeyron-like relationship in multidecadal changes of extreme short-term precipitation and temperature in Japan. *Atmospheric Science Letters*, *14*(3), 127–132. https://doi.org/10.1002/asl2.428

Fujita, M., & Sato, T. (2017). Observed behaviours of precipitable water vapour and precipitation intensity in response to upper air profiles estimated from surface air temperature. *Scientific Reports*, *7*(1), 4233–4210. https://doi.org/10.1038/s41598-017-04443-9

Golroudbary, V. R., Zeng, Y., Mannaerts, C. M., & Su, Z. (Bob). (2019). Response of extreme precipitation to urbanization over the Netherlands. *Journal of Applied Meteorology and Climatology*, *58*(4), 645–661. https://doi.org/10.1175/JAMC-D-18-0180.1

Haerter, J. O., & Berg, P. (2009). Unexpected rise in extreme precipitation caused by a shift in rain type? *Nature Geoscience*, *2*(6), 372–373. https://doi.org/10.1038/ngeo523

Hansen, E., Fenn, D., Schreiner, L., Stodt, R., & Miller, J. (1988). *Probable maximum precipitation estimates*. United States National Weather Service.

Hao, L., & Naiman, D. (2007). *Quantile regression*. Thousand Oaks, CA: SAGE Publications, Inc. https://doi.org/10.4135/9781412985550

Hardwick Jones, R., Westra, S., & Sharma, A. (2010). Observed relationships between extreme sub-daily precipitation, surface temperature, and relative humidity. *Geophysical Research Letters*, *37*, L22805. https://doi.org/10.1029/2010GL045081

Hettiarachchi, S., Wasko, C., & Sharma, A. (2018). Increase in flood risk resulting from climate change in a developed urban watershed—The role of storm temporal patterns. *Hydrology and Earth System Sciences*, *22*(3), 2041–2056. https://doi.org/10.5194/hess-22-2041-2018

Johnson, F., & Sharma, A. (2009). Measurement of GCM skill in predicting variables relevant for hydroclimatological assessments. *Journal of Climate*, *22*(16), 4373–4382. https://doi.org/10.1175/2009JCLI2681.1

Kendon, E. J., Roberts, N. M., Fowler, H. J., Roberts, M. J., Chan, S. C., & Senior, C. A. (2014). Heavier summer downpours with climate change revealed by weather forecast resolution model. *Nature Climate Change*, *4*(July), 570–576. https://doi.org/10.1038/NCLIMATE2258

Koenker, R., & Bassett, G. (1978). Regression Quantiles. *Econometrica*, *46*(1), 33. https://doi.org/10.2307/1913643

Kunkel, K. E., Karl, T. R., Easterling, D. R., Redmond, K., Young, J., Yin, X., & Hennon, P. (2013). Probable maximum precipitation and climate change. *Geophysical Research Letters*, *40*, 1402–1408. https://doi.org/10.1002/grl.50334

Lenderink, G., Barbero, R., Loriaux, J. M., & Fowler, H. J. (2017). Super-Clausius-Clapeyron scaling of extreme hourly convective precipitation and its relation to large-scale atmospheric conditions. *Journal of Climate*, *30*(15), 6037–6052. https://doi.org/10.1175/JCLI-D-16-0808.1

Lenderink, G., Mok, H. Y., Lee, T. C., & van Oldenborgh, G. J. (2011). Scaling and trends of hourly precipitation extremes in two different climate zones—Hong Kong and the Netherlands. *Hydrology and Earth System Sciences*, *15*(9), 3033–3041. https://doi.org/10.5194/hess-15-3033-2011

Lenderink, G., & Attema, J. (2015). A simple scaling approach to produce climate scenarios of local precipitation extremes for the Netherlands. *Environmental Research Letters*, *10*(8), 85,001. https://doi.org/10.1088/1748-9326/10/8/085001

Lenderink, G., & van Meijgaard, E. (2008). Increase in hourly precipitation extremes beyond expectations from temperature changes. *Nature Geoscience*, *1*(8), 511–514. https://doi.org/10.1038/ngeo262

Lenderink, G., & van Meijgaard, E. (2010). Linking increases in hourly precipitation extremes to atmospheric temperature and moisture changes. *Environmental Research Letters*, *5*(2), 025208. https://doi.org/10.1088/1748-9326/5/2/025208

Lochbihler, K., & Lenderink, G. (2017). The spatial extent of rainfall events and its relation to precipitation scaling. *Geophysical Research Letters*, *44*, 8629–8636. https://doi.org/10.1002/2017GL074857

Manola, I., van den Hurk, B., de Moel, H., & Aerts, J. C. J. H. (2018). *Future extreme precipitation intensities based on a historic event* (pp. 3777–3788).

Monteith, J., & Unsworth, M. H. (2008). *Principles of environmental physics*. New York, NY: Elsevier.

Panthou, G., Mailhot, A., Laurence, E., & Talbot, G. (2014). Relationship between surface temperature and extreme rainfalls: A multi-time-scale and event-based analysis. *Journal of Hydrometeorology*, *15*(5), 1999–2011. https://doi.org/10.1175/jhm-d-14-0020.1

Park, I.-H., & Min, S.-K. (2017). Role of convective precipitation in the relationship between subdaily extreme precipitation and temperature. *Journal of Climate*, *30*(23), 9527–9537. https://doi.org/10.1175/jcli-d-17-0075.1

Peleg, N., Marra, F., Fatichi, S., Molnar, P., Morin, E., Sharma, A., & Burlando, P. (2018). Intensification of convective rain cells at warmer temperatures observed from high-resolution weather radar data. *Journal of Hydrometeorology*, *19*(4), 715–726. https://doi.org/10.1175/jhm-d-17-0158.1

Pendergrass, A. G., & Hartman, D. L. (2014). Changes in the distribution of rain frequency and intensity in response to global warming*. *Journal of Climate*, *27*(22), 8372–8383. https://doi.org/10.1175/JCLI-D-14-00183.1

Pendergrass, B. A. G. (2018). What precipitation is extreme? *Global and Planetary Change*, *360*(6393), 1072–1074.

Roderick, T. P., Wasko, C., & Sharma, A. (2019). Atmospheric moisture measurements explain increases in tropical rainfall extremes. *Geophysical Research Letters*, *46*, 1375–1382. https://doi.org/10.1029/2018GL080833

Sharma, A., & Mehrotra, R. (2014). An information theoretic alternative to model a natural system using observational information alone. *Water Resources Research*, *50*, 650–660. https://doi.org/10.1002/2013WR013845

Sharma, A., Mehrotra, R., Li, J., & Jha, S. (2016). A programming tool for nonparametric system prediction using partial informational correlation and partial weights. *Environmental Modelling and Software*, *83*, 271–275. https://doi.org/10.1016/j.envsoft.2016.05.021

Shi, F., Hao, Z., & Shao, Q. (2014). The analysis of water vapor budget and its future change in the Yellow-Huai-Hai region of China. *Journal of Geophysical Research: Atmospheres*, *119*, 6140–6159. https://doi.org/10.1002/2014JD021606

Soden, B. J., & Held, I. M. (2006). An assessment of climate feedbacks in coupled ocean-atmosphere models. *Journal of Climate*, *19*(23), 6263–3360. https://doi.org/10.1175/JCLI9028.1

Tobin, D. C., Revercomb, H. E., Knuteson, R. O., Lesht, B. M., Strow, L. L., Hannon, S. E., et al. (2006). Atmospheric radiation measurement site atmospheric state best estimates for Atmospheric Infrared Sounder temperature and water vapor retrieval validation. *Journal of Geophysical Research*, *111*, D09S14. https://doi.org/10.1029/2005JD006103

Trenberth, K. E. (1999). Conceptual framework for changes of extremes of the hydrological cycle with climate change. *National Center for Atmospheric Research*, *42*, 327–339.
Trenberth, K. E. (2011). Changes in precipitation with climate change. *Climate Research*, *47*(1), 123–138. https://doi.org/10.3354/cr00953
Trenberth, K. E., Dai, A., Rasmussen, R. M., & Parsons, D. B. (2003). The changing character of precipitation. *Bulletin of the American Meteorological Society*, *84*(9), 1205–1218. https://doi.org/10.1175/BAMS-84-9-1205
Trenberth, K. E., & Shea, D. J. (2005). Relationships between precipitation and surface temperature. *Geophysical Research Letters*, *32*, L14703. https://doi.org/10.1029/2005GL022760
Utsumi, N., Seto, S., Kanae, S., Maeda, E. E., & Oki, T. (2011). Does higher surface temperature intensify extreme precipitation? *Geophysical Research Letters*, *38*, L16708. https://doi.org/10.1029/2011GL048426
Verstraten, L., Wasko, C., Ashford, G., & Sharma, A. (2019). Sensitivity of Australian roof drainage structures to design rainfall variability and climatic change. *Building and Environment*, *161*(April), 106230. https://doi.org/10.1016/j.buildenv.2019.106230
Wang, G., Wang, D., Trenberth, K. E., Erfanian, A., Yu, M., Bosilovich, M. G., & Parr, D. T. (2017). The peak structure and future changes of the relationships between extreme precipitation and temperature. *Nature Climate Change*, *7*(4), 268–274. https://doi.org/10.1038/nclimate3239
Wasko, C., Lu, W. T., & Mehrotra, R. (2018). Relationship of extreme precipitation, dry-bulb temperature, and dew point temperature across Australia. *Environmental Research Letters*, *13*(7), 074031. https://doi.org/10.1088/1748-9326/aad135
Wasko, C., Parinussa, R. M., & Sharma, A. (2016). A quasi-global assessment of changes in remotely sensed rainfall extremes with temperature. *Geophysical Research Letters*, *43*, 12,659–12,668. https://doi.org/10.1002/2016GL071354
Wasko, C., & Nathan, R. (2019). The local dependency of precipitation on historical changes in temperature. *Climatic Change*, *156*(1–2), 105–120. https://doi.org/10.1007/s10584-019-02523-5
Wasko, C., & Sharma, A. (2014). Quantile regression for investigating scaling of extreme precipitation with temperature. *Water Resources Research*, *50*, 3608–3614. https://doi.org/10.1002/2013WR015194
Wasko, C., & Sharma, A. (2017a). Continuous rainfall generation for a warmer climate using observed temperature sensitivities. *Journal of Hydrology*, *544*, 575–590. https://doi.org/10.1016/j.jhydrol.2016.12.002
Wasko, C., & Sharma, A. (2017b). Global assessment of flood and storm extremes with increased temperatures. *Scientific Reports*, *7*(1), 7945. https://doi.org/10.1038/s41598-017-08481-1
Westra, S., Alexander, L. V., & Zwiers, F. W. (2013). Global increasing trends in annual maximum daily precipitation. *Journal of Climate*, *26*(11), 3904–3918. https://doi.org/10.1175/JCLI-D-12-00502.1
Westra, S., Evans, J. P., Mehrotra, R., & Sharma, A. (2013). A conditional disaggregation algorithm for generating fine time-scale rainfall data in a warmer climate. *Journal of Hydrology*, *479*, 86–99. https://doi.org/10.1016/j.jhydrol.2012.11.033
Westra, S., Fowler, H. J., Evans, J. P., Alexander, L. V., Berg, P., Johnson, F., et al. (2014). Future changes to the intensity and frequency of short-duration extreme rainfall. *Reviews of Geophysics*, *69*, 849–555. https://doi.org/10.1029/88EO01108
Woldemeskel, F. M., Sharma, A., Sivakumar, B., & Mehrotra, R. (2015). Quantification of precipitation and temperature uncertainties simulated by CMIP3 and CMIP5 models. *Journal of Geophysical Research: Atmospheres*, *12*, 3–17. https://doi.org/10.1002/2015JD023719. Received
Zhang, W., Villarini, G., & Wehner, M. (2019). *Contrasting the responses of extreme precipitation to changes in surface air and dew point temperatures* (pp. 257–271).
Zhang, X., Zwiers, F. W., Li, G., Wan, H., & Cannon, A. J. (2017). Complexity in estimating past and future extreme short-duration rainfall. *Nature Geoscience*, *10*(4), 255–259. https://doi.org/10.1038/ngeo2911
Zwiers, V. V., Zwiers, F. W., Zhang, X., & Wehner, M. (2013). Changes in temperature and precipitation extremes in the CMIP5 ensemble. *Climatic Change*, *119*(2), 345–357. https://doi.org/10.1007/s10584-013-0705-8